# Removal of Acid Brown 354 from wastewater by aminized cellulose acetate nanofibers: experimental and theoretical study of the effect of different parameters on adsorption efficiency

Mehran Namjoufar, Ali Farzi and Afzal Karimi

## ABSTRACT

Wastewater effluents usually involve dyes that are dangerous for aquatic life and other environments. Many of these dyes are toxic, carcinogenic, and can cause skin and eye irritation. In this study, firstly aminized cellulose acetate was prepared from cellulose acetate and applied for the adsorption of Acid Brown 354 from aqueous solutions. The effects of different parameters including adsorbent dosage, pH, temperature, and initial concentration of dye on adsorption capacity were examined. Results showed that removal efficiency of dye declined by increasing values of all parameters. Finally, maximum removal of dye was achieved in the presence of 0.1 g adsorbent, pH of 2, and 10 mg/L of initial dye concentration at a temperature of 25 °C. Also, different adsorption isotherms were investigated including Langmuir, Temkin, and Freundlich models and results demonstrated that the adsorption isotherm of dye followed the Freundlich model with a correlation coefficient of 0.988 revealing that the bond between the dye and the adsorbent is strong. Finally, kinetic study indicated that the adsorption of dye is exactly governed by pseudo-second-order kinetics explaining that the adsorption process is chemical and the adsorbent can not be reused.

**Key words** | Acid Brown 354, adsorption isotherm, aminized cellulose acetate, dye removal, kinetic modeling

**Mehran Namjoufar**
**Ali Farzi** (corresponding author)
Department of Chemical Engineering, Faculty of Chemical and Petroleum Engineering,
University of Tabriz,
Tabriz,
Iran
E-mail: *a-farzi@tabrizu.ac.ir*

**Afzal Karimi**
Faculty of Advanced Technologies in Medicine,
Iran University of Medical Sciences,
Tehran 1449614535,
Iran

## HIGHLIGHTS

- Synthesis of aminized cellulose acetate nanofibers (ACA) with hydrophilic and alkaline properties.
- Removal of Acid Brown 354 dye by ACA nanofibers and studying the effect of different parameters.
- Investigation of equilibrium isotherms and equilibrium thermodynamic parameters and introducing the best isotherm model.
- Study of kinetics and mechanism of the dye removal process and proposing the best kinetic model.



doi: 10.2166/wst.2021.070

## INTRODUCTION

Industrial wastes, which usually include different kinds of dyes and other pollutants, are one of the major causes of contamination of water resources. Dyes are colorful substances that are widely used in printing, textile, plastics, leather tanning, food, pharmaceuticals, cosmetics, pigment, and many other industries (Ahmad *et al.* 2015; Seow & Lim 2016; Katheresan *et al.* 2018; Ruan *et al.* 2019). Dye pollutants can endanger aquatic life as they are naturally toxic. Therefore, their entrance into water resources is unacceptable and should be prevented by different removal methods (Katheresan *et al.* 2018).

Due to the environmental and health concerns associated with wastewater effluents, a wide range of techniques has been developed and utilized for removing dyes, which can be classified into three main categories of chemical, physical, and biological techniques (Seow & Lim 2016). Some of these conventional techniques include membrane filtration, coagulation and flocculation, sedimentation, chemical precipitation, ion exchange, and adsorption (Wu *et al.* 2008; Chen *et al.* 2009; Rajasulochana & Preethy 2016; Teh *et al.* 2016; Ali *et al.* 2018; Saleh *et al.* 2018; Dharupaneedi *et al.* 2019; Ejraei *et al.* 2019; Ruan *et al.* 2019). Adsorption, as a combination of physical-chemical methods, is found to be the most favorable and economic method to eliminate dye pollutants from wastewater (Nasar & Shakoor 2017; Saber-Samandari *et al.* 2017; Guo *et al.* 2018). This method has been widely accepted as one of the most effective effluent treatment techniques for removing hazardous inorganic and organic pollutants because it is fast, inexpensive, efficient, and easy to design (Raval *et al.* 2016; Nasar & Mashkoor 2019). An ideal adsorbent for dye elimination should have some favorable features such as high adsorption capacity, large surface area, high porosity, easy availability, mechanical stability, environmental friendliness, compatibility, ease of recovery, and high selectivity to remove a wide range of dyes (Yagub *et al.* 2014). Finding a highly efficient sorbent substance is the most important issue for practical utilization of the adsorption method.

Bhowmik *et al.* (2018) investigated the performance of $Fe_2O_3/Mn_3O_4$ nanocomposite for the removal of methyl orange (MO) from aqueous solutions. They reported that the maximum removal efficiency of MO was achieved at pH of 2.0 and ranged between 70.35 to 98.78% for different sorbent doses of 0.25 to 1.0 g/L, with an initial dye concentration of 100 mg/L. Konicki *et al.* (2018) assessed the efficiency of $ZnO/ZnMn_2O_4$ composite for the removal of basic yellow 28 (BY 28) from aqueous solutions. They reported that the amount of dye adsorbed was improved by increasing the solution pH, where an increase in pH from 3.4 to 11 resulted in the increase of dye adsorption capacity from 36.4 to 55.4 mg/g. Also, they investigated the effect of initial dye concentration on adsorption efficiency and demonstrated that its increase from 10 to 50 mg/L leads to the increase of adsorption capacity from 25.9 to 44 mg/g at pH of 7.0 and temperature of 30 °C. Fazlzadeh *et al.* (2016) investigated removal of acid black dye from aqueous solutions using magnetite nanoparticles. Their results showed that by decreasing the initial pH of the solution and the adsorbent concentration, the adsorption capacity of nanoparticles was increased, while increasing temperature and/or concentration decreased removal efficiency. The highest removal efficiency was achieved for the initial adsorbent concentration of 25 mg/L at pH of 2, reaction time of 60 min, and nanoparticle concentration of 1.2 g/L which was 98%.

Song *et al.* (2008) investigated removal of Acid Brown 348 from aqueous solutions using ultrasound-assisted adsorption on exfoliated graphite. They examined the effect of different parameters such as temperature, contact time, pH, etc. The yield of their proposed method was 90% within 120 min at 40 °C and pH of 1 using 2 g/L of the adsorbent. Pandima Devi & Muthukumaran (2013) focused on adsorption kinetics of Acid Brown 48 from aqueous solutions using chicken feathers as biowaste. Equilibrium conditions were established after 24 h of contact time at optimum pH of 2 and confirmed that both Freundlich and Langmuir isotherms can predict adsorption isotherms with good accuracy. Kałużna–Czaplińska *et al.* (2010) utilized an advanced oxidization method for the degradation of $1 \times 10^{-4}$ M aqueous solution of C.I. Acid Brown 349. They used hydrogen peroxide and sodium hypochlorite together with different concentrations of $Fe^{2+}$ ions and obtained 100% removal efficiency under optimum conditions; for example, at pH of 2.5. Pansuk & Vinitnantharat (2011) studied adsorption of Acid Brown 75 and Direct Yellow 162 from aqueous solutions using unmodified fly ash and surfactant-modified granules. They investigated the adsorption capacities of the adsorbents at different contact times, temperatures, and adsorbent concentrations, and found that by increasing temperature, the adsorption capacity increased, which revealed that the adsorption process of anionic dyes is endothermic. Dehghan Abkenar (2018)

studied removal of Acid Brown 214 from water solution using fluorene functionalized nanoporous SBA-15 adsorbent. She synthesized the adsorbent and performed different analyses to identify the structural characteristics of the adsorbent. Then she used the synthesized adsorbent for the removal of Acid Brown 214 with a concentration of 50 mg/L and found that the maximum adsorption capacity was achieved at pH value of 4 after 5 min of contact time. Also, kinetic study showed that the adsorption process follows pseudo-second order kinetics. Hassan *et al.* (2020) investigated removal of Acid Brown 354 using *Haloxylon recurvum* stem biomass as the adsorbent. They found that the high removal was obtained at acidic pH of 2 with minimum contact time of 20 min. Also, increasing temperature decreased removal efficiency. Their kinetic study showed that the removal process follows pseudo-second order kinetics and isotherms of Langmuir and Temkin best fitted the equilibrium results.

Recently, 3-Chloro-2-Hydroxypropyl Trimethyl Ammonium Chloride (CHPTAC) has attracted much attention in the cationization of cellulose because of commercial availability, good reactivity, and low toxicity (Hashem 2006; Pal *et al.* 2006). For example, Li *et al.* (2015) prepared a cationic cellulose derivative, cellulose-CHPTAC, by homogeneous etherification of cellulose with CHPTAC in a NaOH/urea aqueous solution and used it as filler/modifier. Also, Morantes *et al.* (2019) used CHPTAC agent as a cationic graft on cellulose nanocrystals, to form a novel water treatment flocculant. In another study, Golizadeh *et al.* (2019) reported modification of electrospun cellulose nanofibers using CHPTAC monochloroacetic acid. One of the modified nanofibers that they fabricated was Aminized (cationic) Cellulose Acetate (ACA) which is also used in this study as an adsorbent.

In this study, ACA was used to adsorb and remove Acid Brown 354 (AB354) from aqueous solutions. Then, the effects of different parameters including pH, initial concentration of dye, amount of adsorbent, and temperature on dye removal efficiency were investigated. Also, equilibrium studies on adsorption isotherms were performed to find the best model for describing the adsorption mechanism. Furthermore, kinetic modeling of the adsorption process was carried out to determine the rate of adsorption at different conditions, and the adsorption mechanism.

Based on the above literature review and according to our knowledge, no study has been conducted until now for the removal of AB354 dye from aqueous solutions using ACA adsorbent. In this work, it is shown that the utilized adsorbent can adsorb high amounts of the AB354 dye.

## MATERIALS AND METHODS

Table 1 shows all material together with their chemical formula, molar mass, and suppliers used in this study for the removal of AB354.

### Synthesis of aminized cellulose acetate

Firstly, 0.5 g of 1 M NaOH, 8 g of distilled water, 30 g of ethanol (96%), 28 g of CHPTAC, and 5 g of cellulose acetate (CA) were simultaneously poured into a 250 mL Erlenmeyer flask and then the flask was placed on a thermal-magnetic stirrer (Farashafaq, Iran) at a temperature of 70 °C for 30 minutes. The desired temperature was observed and controlled manually by a thermometer. Then, the insoluble contents in the flask were filtered through a filter paper (Whatman Ashless, UK). Finally, filtered contents were placed in an oven (BF120E, Iran) for 2 hours to dry the sample at 45 °C.

In this work, cellulose acetate was modified by two sequential wet-on-wet baths process. In first step, CHPTAC instantly converted to 2,3-epoxypropyl trimethylammonium chloride (EPTMAC), and then EPTMAC reacted with CA to form aminized cellulose acetate (ACA) nano-fibers (Figure 1) (Golizadeh *et al.* 2019).

The chemical structure of both CA and ACA nanofibers was analyzed by FTIR method in order to identify functional groups and changes in the chemical structure of CA nanofibers and new functional groups generated due to modification. As FTIR spectra give functional groups and elements of those groups, no other analysis method is needed for chemical structure analysis of ACA nanofibers.

**Table 1** | Chemical formula, molar mass, and suppliers of used materials

| Compound name | Chemical formula | Molar mass (g/mol) | Company |
|---|---|---|---|
| Cellulose acetate | $C_{164}H_{174}O_{111}$ | 3,921 | Merck |
| 3-Chloro-2-hydroxypropyl trimethylammonium chloride | $C_6H_{15}ClNOCl$ | 188.1 | Merck |
| Acid Brown 354 | $C_{30}H_{20}N_8Na_2O_{12}S_2$ | 794.6 | Merck |
| Sodium hydroxide | NaOH | 40.00 | Merck |
| Hydrochloric acid | HCl | 36.46 | Merck |
| Ethanol | $C_2H_5OH$ | 46.07 | Merck |
| Distilled water | $H_2O$ | 18.02 | – |

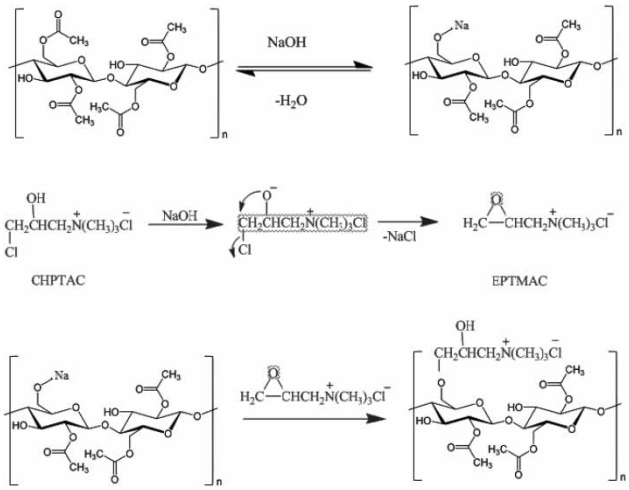


**Figure 1** | Mechanism of modification of cellulose acetate with CHPTAC in basic solution (Golizadeh *et al.* 2019).

FESEM images presented in the work of Golizadeh *et al.* (2019) revealed that ACA nanofibers have a smooth surface. Also, average diameters of nanofibers were reported in that work. Because the synthesis procedure was from the mentioned work, therefore no more analysis was needed for investigation of the physical structure of the synthesized nanofibers. Only FTIR analysis was done in this work in order to make sure that the procedure of ACA fabrication was correct.

## Acid Brown 354 azo dye

AB354 dye with the chemical formula of $C_{30}H_{20}N_8Na_2O_{12}S_2$ is an acidic azo dye with a red light brown color and is used for wool dyeing and printing, and leather shading (Hassan *et al.* 2020). The structural formula of the dye is shown in Figure 2.

Due to the acidic nature of the dye, an adsorbent with alkaline nature can remove the dye more effectively. ACA nanofibers are insoluble in water and due to the alkaline nature of the amine group it can be a good candidate for the removal of AB354. The preparation method of the adsorbent used in this study is easy and cheap, which are its advantages over other conventional adsorbents.

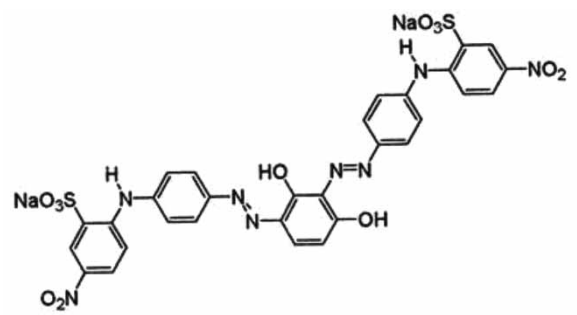


**Figure 2** | Structural formula of Acid Brown 354 azo dye (dye|World dye variety 2020).

## Dye adsorption experiments

Aqueous supply solutions (1,000 ppm) of AB354 dye were prepared by dissolving 1 g of solid dye in 1,000 mL of deionized water. Then, working solutions with different concentrations of dye were prepared by consecutive dilution of the stock solution with distilled water. For example, to prepare a working solution containing 2 ppm (mg/L) of dye, 2 mL of the supply solution containing 1,000 ppm of dye was taken and poured into a container and the volume of the liquid within it was augmented to 1 L by adding deionized water. Calibration curves were plotted using the absorbance values of the standard solutions at concentrations of 0.5, 1.5, 2, 4, 6, 8, 10 mg/L at maximum wavelength of 440 nm using a UV-Vis spectrophotometer (Photonix, Denmark) (El-Ashtoukhy *et al.* 2012) (Figure 3).

To study the performance of aminized cellulose acetate, adsorption of dye from contaminated waters were performed and concentrations of remaining acid brown 354 were measured at maximum wavelength of 440 nm based on the calibration curve. Batch adsorption experiments were performed by contacting 0.1 g of the adsorbent with desired concentrations (10–150 ppm) of dye in 100 mL of aqueous solution at a temperature of 25 °C and pH of 7 for 60 min as base values of the parameters. After 10 min, the suspension was centrifuged and the concentration of AB354 adsorbed on ACA nanofibers was determined by the method described above. The equilibrium adsorption capacity $q_e$ (mg/g) and removal rate ($R$ %) were calculated

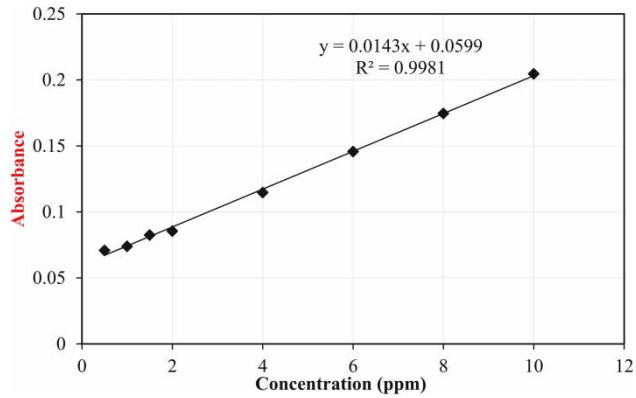


**Figure 3** | Calibration of Acid Brown 354 solutions at wavelength of 440 nm.

according to the following equations:

$$q_e = \frac{(C_0 - C_e)V}{m} \quad (1)$$

$$R\% = \frac{(C_0 - C_e)100}{C_0} \quad (2)$$

where $C_0$ and $C_e$ (mg/L) are initial and equilibrium concentrations of dye, and $m$ (g) and $V$ (L) are the mass of the adsorbent and volume of the dye solution, respectively (Wang *et al.* 2016; Hamedi *et al.* 2019).

In order to identify changes in the structure of Aminized cellulose acetate nanofibers, FTIR analysis was performed using Fourier-transform infrared spectroscopy apparatus (TENSOR 27, Brucker, Germany) and FTIR spectra were obtained and analyzed.

## Adsorption isotherms

The adsorption isotherm is an expression that indicates the equilibrium concentration of adsorbate at the surface of an adsorbent at a constant temperature (Gautam & Chattopadhyaya 2016). Three isotherm models including Freundlich, Langmuir, and Temkin isotherms were applied and equilibrium adsorption data were fitted. The following equations describe these isotherm models (Asnaoui *et al.* 2015; Biftu & Ravindhranath 2020).

Freundlich adsorption isotherm model

$$\ln q_e = \ln k_f + \frac{1}{n}\ln C_e \quad (3)$$

Langmuir adsorption isotherm model

$$\frac{C_e}{q_e} = \frac{1}{k.q_{\max}} + \frac{C_e}{q_{\max}} \quad (4)$$

Temkin adsorption isotherm model

$$q_e = \left(\frac{RT}{b}\right)\ln(K_t C_e) \quad (5)$$

where $C_e$ is the equilibrium dye concentration (mg/L) on an adsorbent surface, $q_e$ is the amount of dye adsorbed at equilibrium (mg/g), $k_f$ is the Freundlich constant (mg/g), $n$ is considered as the heterogeneity of the adsorbent surface and its affinity for the adsorbate, $q_{\max}$ is the maximum adsorption capacity (mg/g), $k$ is the Langmuir constant (L/mg), $K_t$ reveals the equilibrium binding constant (L/mol), $R$ is the universal gas constant (8.314 J/mol.K), and $b$ is linked to the heat of adsorption (Chen *et al.* 2003; Ho *et al.* 2005; Hameed & Rahman 2008; Piccin *et al.* 2011). Equation (3) can be expressed in linear form as below for use in linear regression:

$$q_e = B_T \ln K_t + B_T \ln C_e, \quad B_T = \frac{RT}{b} \quad (6)$$

$B_T$ is related to the heat of sorption and a positive value for it implies that the sorption process is exothermic (Togue Kamga 2018).

In order to calculate constants of isotherms, experiments were repeated at optimum values of the parameters and with different values for the initial concentration of dye in aqueous solutions. The volume of the solution was 100 mL in all experiments. Then, constants of isotherms were calculated using linear regression on experimental data.

## Adsorption kinetics

Kinetic modeling of any reactive process, including adsorption, gives valuable data about the rate of consumption of a component in a process such as a dye, which is essential for designing a continuous or batch processing system for the process. Also, it helps to identify the limiting step, wherein adsorption can be controlled by different mechanisms including complexation, film diffusion, pore diffusion, and ion-exchange processes (Ofomaja 2008; Jarrah & Farhadi 2018). In this study, pseudo-first-order and pseudo-second-order kinetic models were applied to model the dye removal rate. The pseudo-first-order kinetic model states that the adsorption rate is proportional to the number of free adsorption sites. It is represented by the following equation (Mahmoodi *et al.* 2012):

$$\frac{dq_t}{dt} = k_1(q_e - q_t) \quad (7)$$

where, $q_t$ is the amount of dye adsorbed (mg/g) at time $t$ (min), and $k_1$ is the pseudo-first-order rate constant ($\text{min}^{-1}$) (Ho & McKay 1998). Integration of the above equation in the range of [0, t] results:

$$q_t = q_e(1 - e^{-k_1 t}) \quad (8)$$

Reaction curve method (Huang & Jeng 2005) was used for calculation of kinetic parameters of this model. In this method, the slope of the tangent line on the curve at $t = 0$ is related to $k_1$.

$$\left.\frac{dq_t}{dt}\right|_{t=0} = q_e k_1 \quad (9)$$

The other kinetic model that was applied on experimental data was the pseudo-second order rate equation. It assumes that chemisorption is the rate-limiting step and is described as:

$$\frac{dq_t}{dt} = k_1(q_e - q_t)^2 \tag{10}$$

where $k_2$ (g/mg.min) is second order rate constant (Doulia *et al.* 2009). Integration of the above equation with respect to time and re-arranging it will give (Wang *et al.* 2016):

$$\frac{t}{q_t} = \frac{1}{q_e^2 k_2} + \frac{t}{q_e} \tag{11}$$

According to the above equation, the diagram of $t/q_t$ with respect to time should give a straight line if pseudo-second order kinetics hold, and $q_e$ and $k_2$ can be determined from the slope and intercept of the diagram, respectively (Wang *et al.* 2016).

## RESULTS AND DISCUSSION

### FTIR analysis

FTIR spectra were taken for both CA and ACA nanofibers to identify their functional groups and changes in chemical structure of CA during fabrication of ACA nanofibers and to investigate the presence of functional groups on the chemically-modified surface by CA (Figure 4). As indicated in Figure 4(a), vibrations of the acetate group are observed at 1,734 $cm^{-1}$ (C = O, carbonyl stretch), 1,380 $cm^{-1}$ (methyl C-H symmetric/asymmetric bend), and 1,131 $cm^{-1}$ (C-O-C, alkoxyl ester stretch). Also, a broad absorption band at 3,300–3,500 $cm^{-1}$ corresponding to stretching of OH group was observed (Saleh 2011, 2018). The absorption band at 2,700–2,900 $cm^{-1}$ is related to $-CH_2$ groups (Pielesz & Biniaś 2010; Kamal *et al.* 2014). Figure 4(b) depicts the spectrum of ACA, where new bands are observed at 1,021–1,161 $cm^{-1}$, which belong to the stretching vibrations of ammonium groups. In addition, the peaks at 1,453 and 2,921 $cm^{-1}$ are associated with the stretching and bending vibrational states of methylammonium groups, respectively.

### Effects of operating parameters

In this study, the method of one-factor-at-a-time was used for better assessment of each parameter (Frey *et al.* 2003). In this method, all variables except the desired one were kept constant during each experiment and only the desired factor was changed to find its optimum value with the objective of maximum dye removal. The starting conditions were selected as solution volume of 100 mL, pH of 7, dye concentration of 10 ppm, stirring speed of 120 rpm, experiment time of 240 min, and temperature of 25 °C, based on the literature (El-Ashtoukhy *et al.* 2012).

#### Effect of adsorbent dosage

The adsorbent dose is an essential parameter influencing sorption processes by determining the sorption capacity of an adsorbent for a given initial concentration of the adsorbate. For investigating the effect of the amount of adsorbent on dye removal performance, five experiments with different values including 0.1, 0.3, 0.5, 0.7, and 1 g of ACA nanofibers were performed while other parameters were kept constant at their base values. Based on the results shown in Figure 5, the removal percentage of dye decreased by increasing the amount of adsorbent. This observation would be explained considering the fact that the accumulation of adsorbent resulted in decreasing space and concentration of dye molecules within the solution and hence at active sites, and diminishing the removal percentage. The optimum adsorbent dose was observed to be its base value, i.e. 0.1 g, and was applied in further experiments. The maximum removal percentage was obtained as 82.2% at optimum amount of the adsorbent.

#### Effect of pH

The initial pH is also a very significant parameter in the adsorption performance which can influence charges of the adsorbent, ionization/dissociation values of organic pollutants, dissociation of functional groups on the adsorbent active sites, the absorbent surface load, and the dye structure (Lin & Chang 2015; Liu *et al.* 2016). To investigate the effect of pH, five solutions with adsorbent amount of 0.1 g, and pH values of 2, 4, 6, 8 and 10 were prepared by using HCl and NaOH solutions (1 M), while other parameters were kept constant at their base values. According to Figure 6, the removal efficiency of dye at acidic pH values was higher than alkaline ones. At acidic pH values, the surface charge of adsorbent is positive, which attracts negatively charged dye (Kałużna–Czaplińska *et al.* 2010; Pandima Devi & Muthukumaran 2013; Hassan *et al.* 2020) and therefore more AB354 molecules can reach active sites, resulting in the increase of dye removal efficiency. At higher pH values, $OH^-$ ions react with dye making the color of the solution darker brown. Thus, based on the results and

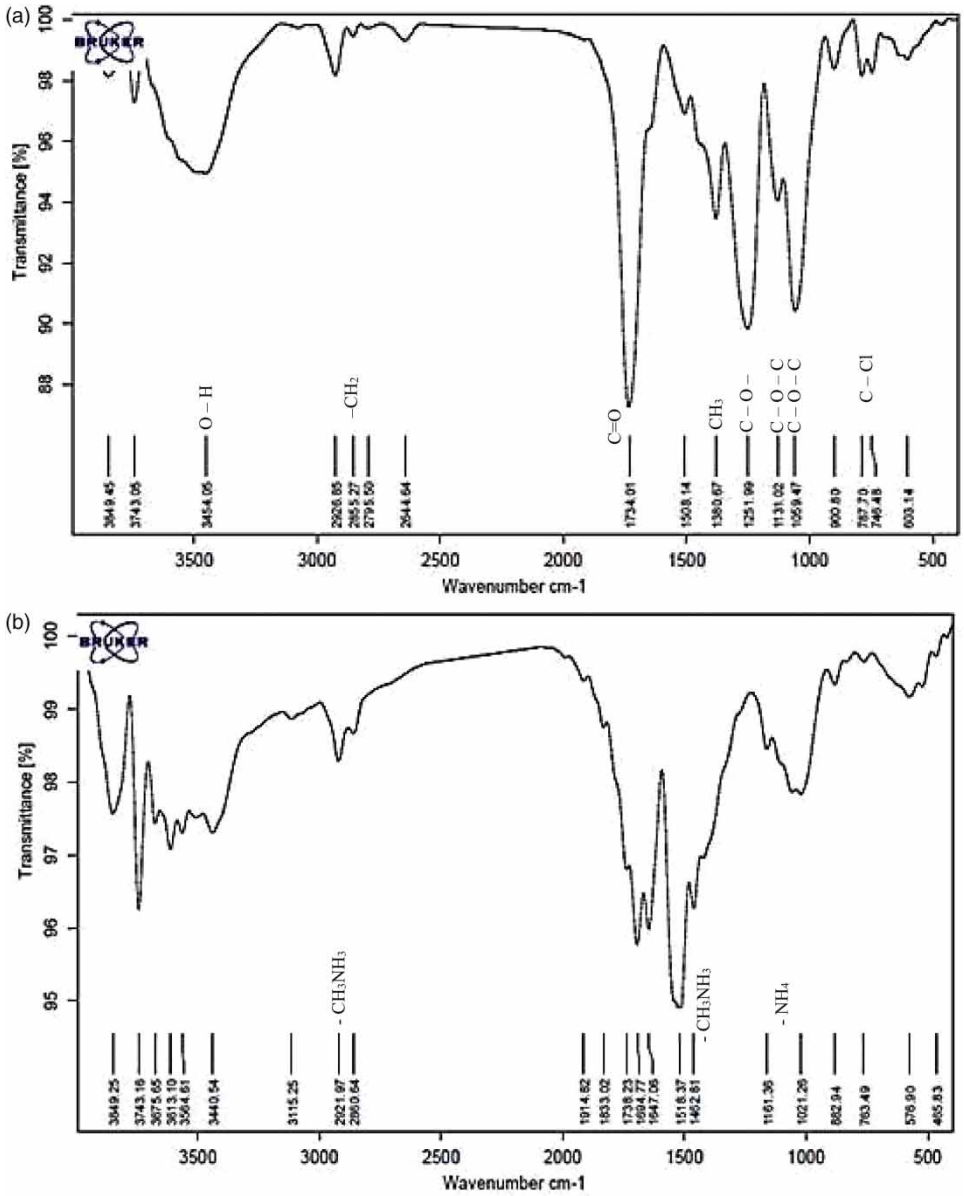


**Figure 4** | FTIR spectra of (a) cellulose acetate and (b) aminized cellulose acetate nanofibers.

considering the above justification, pH value of 2 was selected as optimum for subsequent adsorption studies. This optimum value has also been reported by Hassan *et al.* (2020), which establishes the validity of the experiments at least to this point. As can be seen from Figure 6, removal percentage of the dye at this pH value is 84.53%.

## Effect of initial dye concentration

The initial dye concentration plays an important role in the amount of dye adsorbed by the adsorbent and dye removal efficiency. Usually, increasing initial dye concentration leads to a diminishing percentage of dye removal, which is due to the impregnation of adsorption sites on the adsorbent surface (Salleh *et al.* 2011; Dawood & Sen 2014). To study the effect of this parameter, five dye concentrations of 10, 30, 50, 100, and 150 mg/L were prepared at the optimum pH value of 2 and then mixed with the optimum amount of adsorbent, found earlier. The other parameters were kept constant at their base values. Figure 7 shows the effect of dye concentration on its removal using ACA nanofibers as adsorbent. It is clear that by increasing dye initial

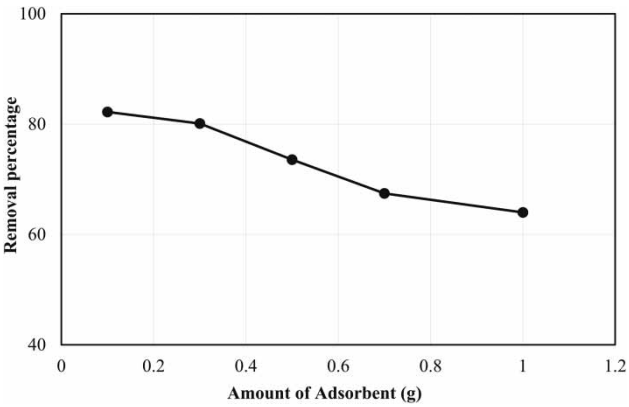


**Figure 5** | Effect of the amount of adsorbent on the removal of AB354 by ACA nanofibers. Experimental conditions: $C_0 = 10$ mg/L, $V = 100$ mL, pH = 7, $T = 25$ °C.

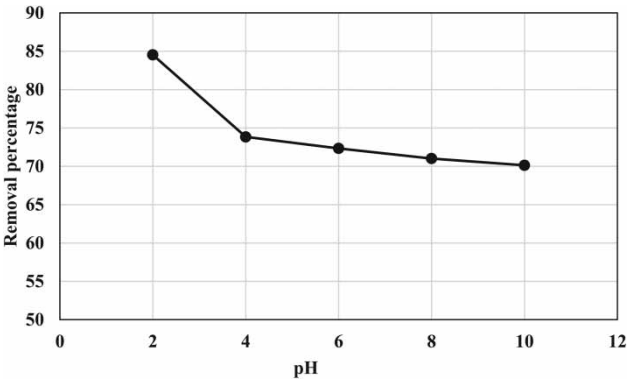


**Figure 6** | Effect of pH on the removal of acid brown 354 by aminized cellulose acetate nanofbers. Experimental conditions: $C_0 = 10$ mg/L, $V = 100$ mL, $m = 0.1$ g, $T = 25$ °C.

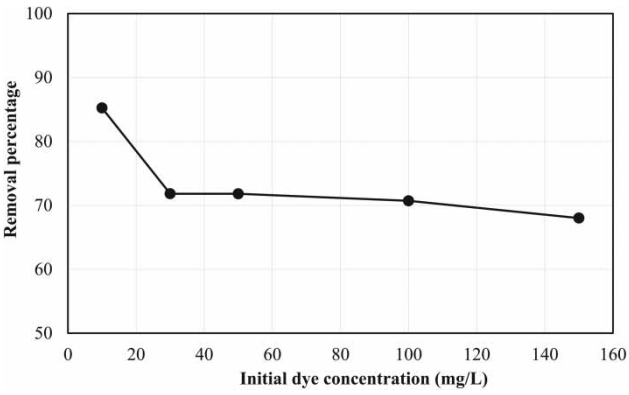


**Figure 7** | Effect of initial dye concentration on the removal of acid brown 354 by aminized cellulose acetate nanofibers. Experimental conditions: $V = 100$ mL, pH = 2, $m = 0.1$ g, $T = 25$ °C.

concentration, its removal percentage decreases which can be attributed to the decreasing and saturation of active sites with the increase of dye concentration. Hassan *et al.* (2020) tested dye concentrations as low as $10^{-4}$ mg/L, which is not comparable with the amounts in this work. As reported in the previous works (Yaseen & Scholz 2019), minimum dye concentration in wastewater is 10 mg/L, which has been tested in this work. Furthermore, dye concentrations as high as 150 mg/L were also tested to show the effectiveness of ACA nanofibers for the removal of this dye. Based on the results shown in Figure 7, an initial dye concentration of 10 mg/L was reported as the optimum value for subsequent experiments. The removal percentage at this value was obtained as 85.24%.

## Effect of temperature

Adsorption temperature also plays a significant role in the removal efficiency of dye. Based on the literature, if adsorption capacity improves with decreasing temperature, the adsorption process is exothermic (Dawood & Sen 2014; Hassan *et al.* 2020). In this study, the effect of temperature was investigated at four values of 25, 30, 40, and 50 °C while other factors were kept constant at their optimum values. As can be seen from Figure 8, the removal percentage has been decreased with temperature increase, which indicates dye adsorption is an exothermic process (Dawood & Sen 2014; Hassan *et al.* 2020). This result indicates that the adsorption process is spontaneous, because in this case there is a decrease in enthalpy and Gibbs free energy of the system. According to the following equation:

$$\Delta G^{\circ} = -RT \ln K_d, \quad K_d = \frac{C_0 - C_e}{C_e} = \frac{R}{1 - R} \tag{12}$$

where $K_d$ is the equilibrium constant. According to the above equation, for removal percentages greater than 50%

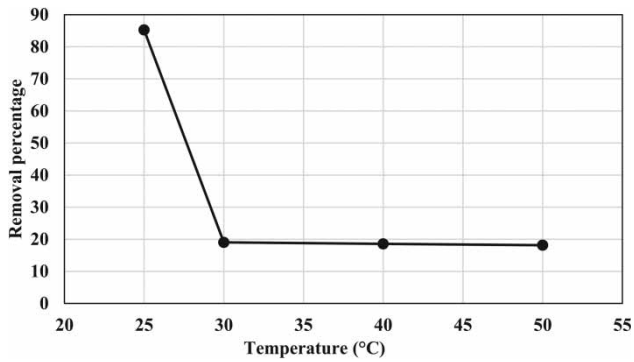


**Figure 8** | Effect of temperature on the removal of acid brown 354 by aminized cellulose acetate nanofibers. Experimental conditions: $C_0 = 10$ mg/L, $V = 100$ mL, pH = 2, $m = 0.1$ g.

$K_d > 1$ which is the case in all of the experiments and therefore $\Delta G^\circ$ is always negative for the adsorption of AB354 dye by the adsorbent, which implies that the adsorption process is spontaneous.

Based on the results, the best reaction temperature was considered as 25 °C, which is equal to the optimum value reported by Hassan *et al.* (2020).

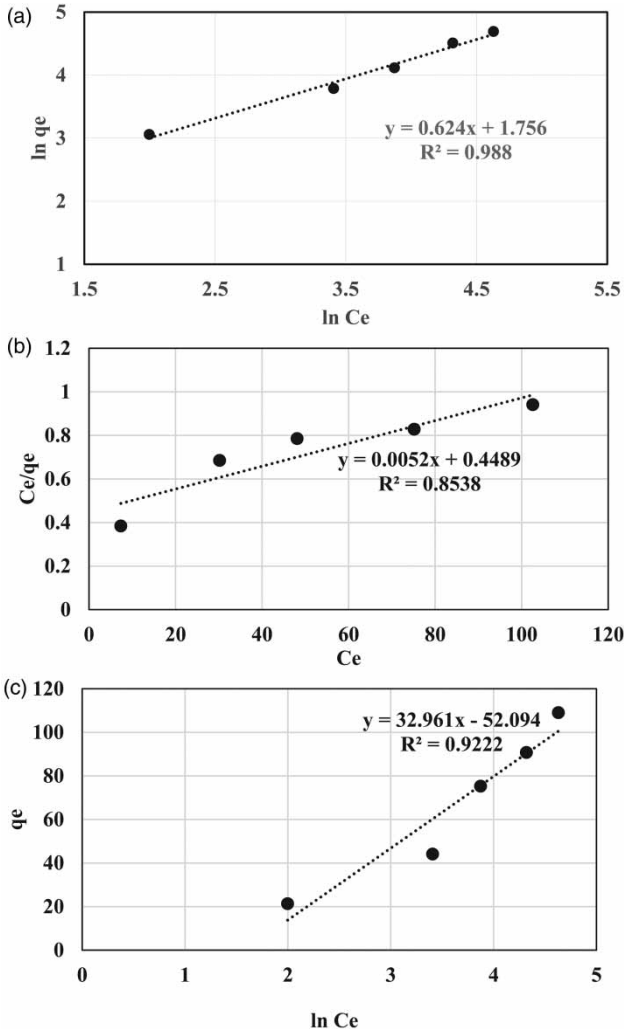


**Figure 9** | Isotherm plots for (a) Freundlich, (b) Langmuir, and (c) Temkin obtained for fitting dye removal by aminized cellulose acetate nanofibers. Experiment conditions: $V = 100$ mL, pH = 2, $m = 0.1$ g, $T = 25$ °C and different initial concentrations of dye.

Based on the experimental results and optimum values of different parameters reported here, the maximum removal percentage was obtained as 85.24% with the adsorbent amount of 0.1 g, and initial dye concentration of 10 mg/L at pH of 2 and solution temperature of 25 °C.

## Modeling of adsorption isotherms

The experimental adsorption isotherm data of AB354 on the surface of aminized cellulose acetate are shown in Figure 9. As was mentioned before, different experiments were conducted at optimum values of the parameters, with different values for the initial concentration of dye while the volume of the solution was 100 mL. Constants of isotherms were calculated using linear regression on experimental data for the case of different initial dye concentration for each model. Trend lines and fitting equations are shown in Figure 9. Also, correlation coefficients are calculated for three models, which are shown in Table 2 and Figure 9. Considering $R^2$ values of three models, the Freundlich adsorption isotherm fitted experimental data better than the Langmuir and Temkin models, which indicates that the adsorbent surface is heterogeneous and the dye does not form a monolayer on the adsorbent and rather follows multilayer adsorption (Piccin *et al.* 2011; Al-Ghouti & Da'ana 2020). The value of $n$ is larger than unity, which implies that the bond between the dye and absorbent is strong. Also, a positive value is obtained for $B_T$ for the Temkin isotherm model, which means that the process is exothermic.

## Adsorption kinetics

As mentioned in the Materials and Methods section, kinetic modeling was performed on experimental data in order to reveal the kinetics and mechanism of adsorption on the adsorbent. In this study, pseudo-first-order and pseudo-second-order kinetic models were applied to model dye removal rate.

The plot of the pseudo-first order kinetic model for an initial concentration of 10 mg/L of dye and optimum values of other parameters is demonstrated in Figure 10. Kinetic parameters of $k_1$ and $q_e$ can be calculated from the diagram of $q_t$

**Table 2** | Langmuir, Freundlich, and Temkin isotherm constants and their correlation coefficients, calculated based on experimental results.

| Langmuir | | | Freundlich | | | Temkin | | |
|---|---|---|---|---|---|---|---|---|
| $q_{max}$ (mg/g) | $k$ (L/mg) | $R^2$ | $k_f$ (mg/g) | $n$ | $R^2$ | $B_T$ | $K_t$ | $R^2$ |
| 192.3 | 0.012 | 0.854 | 5.785 | 1.602 | 0.988 | 32.96 | 0.206 | 0.922 |

Experiments conditions: $V = 100$ mL, pH = 2, $m = 0.1$ g, $T = 25$ °C and different initial concentrations of dye.

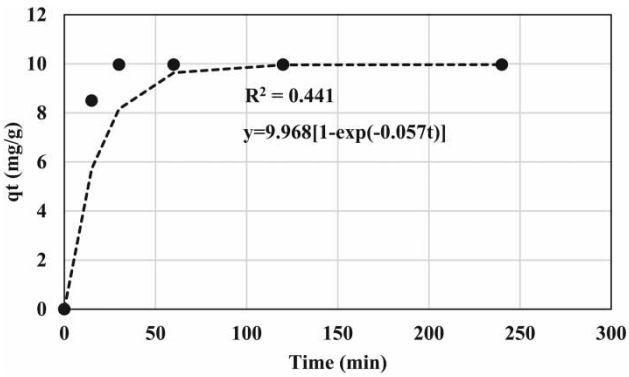


**Figure 10** | Pseudo-first-order kinetic for acid brown 354 adsorption experiments. Experimental conditions: $C_0 = 10$ mg/L, $V = 100$ mL, pH = 2, $m = 0.1$ g, $T = 25$ °C.

versus $t$ (Table 3). As mentioned before, the reaction curve method (Huang & Jeng 2005) was used for calculation of kinetic parameters. As can be seen, the curve fitting reveals a low correlation coefficient of 0.441 and therefore it can be concluded that the adsorption of AB354 by ACA nanofibers does not follow pseudo-first order kinetics.

Also, curve fitting using the pseudo-second order model on experimental data was performed and the plot of $t/q_t$ with respect to time was depicted, which is shown in Figure 11. According to Figure 11, exact linearity has been achieved by utilizing the pseudo-second order model with $R^2 = 1.000$, denoting

**Table 3** | Rate constants and correlation coefficients for acid brown 354 adsorptions with 10 mg/L dye concentration and optimum values of other parameters for pseudo- first and second order kinetic models

| | Pseudo-first order | | | Pseudo-second order | | |
|---|---|---|---|---|---|---|
| $q_{e,\,exp}$ (mg/g) | $k_1$ ($min^{-1}$) | $R^2$ | $q_{e,\,cal}$ (mg/g) | $K_2$ (g/mg.min) | $R^2$ | $q_{e,\,cal}$ (mg/g) |
| 9.968 | $5.685 \times 10^{-2}$ | 0.441 | 9.968 | 0.118 | 1.000 | 9.234 |

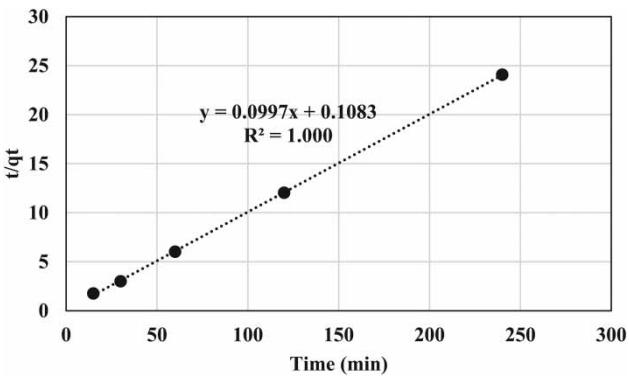


**Figure 11** | Curve fitting with pseudo-second order kinetics for acid brown 354 adsorption experiments. Experimental conditions: $C_0 = 10$ mg/L, $V = 100$ mL, pH = 2, $m = 0.1$ g, $T = 25$ °C.

chemisorption (Doulia *et al.* 2009) which means that the adsorbent cannot be regenerated for further uses. Calculated kinetic parameters for this model are also shown in Table 3.

## CONCLUSIONS

Removal of dyes from wastewater effluents in textile industries is a challenging problem due to the wide range of dyes and their properties. Many investigations are devoted to this area and different methods are applied for the removal of dye. Adsorption is the most widely used and more reliable method compared to other methods. In this study, removal of acid brown 354 dye from aqueous solutions using a modified adsorbent was performed. For this purpose, the surface of cellulose acetate was modified by CHPTAC for fabrication of aminized cellulose acetate nanofibers as an efficient adsorbent for dye removal. Different adsorption experiments were performed to find optimum conditions of effective parameters. Effective parameters on the adsorption capacity including pH, initial dye concentration, adsorbent dosage, and temperature of the solution were studied. The results demonstrated that the maximum removal of acid brown 354 was achieved at 10 mg/L of initial dye concentration with 0.1 g of the adsorbent while optimum pH and temperature were 2 and 25 °C, respectively. Also, equilibrium analysis with different isotherm models was performed and it was revealed that Freundlich isotherm fitted dye removal experimental data better than other models with a correlation coefficient of 0.988, proposing that acid brown 354 does not form a monolayer on the adsorbent and rather follows multilayer adsorption. Also, the obtained value for the exponent of the model was greater than one (1.602), revealing strong bond formation between dye and adsorbent (Al-Ghouti & Da'ana 2020). Furthermore, it was shown by equilibrium studies that the process is spontaneous. Finally, kinetic modeling of the process was performed and it was shown that adsorption kinetics of the dye followed the pseudo-second order kinetic model with exact fitting on experimental data and the model coefficient was found to be 0.118. Because the pseudo-second order kinetic model governs experimental data, it indicates a chemisorption process and thus the adsorbent could not be used again (Doulia *et al.* 2009).

## DATA AVAILABILITY STATEMENT

All relevant data are included in the paper or its Supplementary Information.

## REFERENCES


Ahmad, A., Mohd-Setapar, S. H., Chuong, C. S., Khatoon, A., Wani, W. A., Kumar, R. & Rafatullah, M. 2015 Recent advances in new generation dye removal technologies: novel search for approaches to reprocess wastewater. *RSC Advances* **5** (39), 30801–30818. https://doi.org/10.1039/C4RA16959 J.

Al-Ghouti, M. A. & Da'ana, D. A. 2020 Guidelines for the use and interpretation of adsorption isotherm models: a review. *Journal of Hazardous Materials* **393**, 122383. https://doi.org/10.1016/j.jhazmat.2020.122383.

Ali, I., Al-Hammadi, S. A. & Saleh, T. A. 2018 Simultaneous sorption of dyes and toxic metals from waters using synthesized titania-incorporated polyamide. *Journal of Molecular Liquids* **269**, 564–571. https://doi.org/10.1016/j.molliq.2018.08.081.

Asnaoui, H., Laaziri, A. & Khalis, M. 2015 Study of the kinetics and the adsorption isotherm of cadmium(II) from aqueous solution using green algae (Ulva lactuca) biomass. *Water Science and Technology* **72** (9), 1505–1515. doi:10.2166/wst.2015.359.

Bhowmik, M., Deb, K., Debnath, A. & Saha, B. 2018 Mixed phase $Fe_2O_3/Mn_3O_4$ magnetic nanocomposite for enhanced adsorption of methyl orange dye: neural network modeling and response surface methodology optimization. *Applied Organometallic Chemistry* **32** (3), e4186. https://doi.org/10.1002/aoc.4186.

Biftu, W. K. & Ravindhranath, K. 2020 Synthesis of nano$ZrO_2$ via simple new green routes and its effective application as adsorbent in phosphate remediation of water with or without immobilization in Al-alginate beads. *Water Science and Technology* **81** (12), 2617–2633. doi:10.2166/wst.2020.318.

Chen, J. P., Wu, S. & Chong, K.-H. 2003 Surface modification of a granular activated carbon by citric acid for enhancement of copper adsorption. *Carbon* **41** (10), 1979–1986. https://doi.org/10.1016/S0008-6223(03)00197-0.

Chen, T., Kao, C., Hong, A., Lin, C. & Liang, S. 2009 Application of ozone on the decolorization of reactive dyes – Orange-13 and Blue-19. *Desalination* **249** (3), 1238–1242. https://doi.org/10.1016/j.desal.2008.10.032.

Dawood, S. & Sen, T. 2014 Review on dye removal from its aqueous solution into alternative cost effective and non-conventional adsorbents. *Journal of Chemical and Process Engineering* **1** (104), 1–11.

Dehghan Abkenar, S. 2018 Fast and efficient removal of Acid Brown 214 from aqueous media by adsorption onto fluorene functionalized nanoporous SBA-15. *Indian Journal of Chemical Technology* **25**, 376–382.

Dharupaneedi, S. P., Nataraj, S. K., Nadagouda, M., Reddy, K. R., Shukla, S. S. & Aminabhavi, T. M. 2019 Membrane-based separation of potential emerging pollutants. *Separation and Purification Technology* **210**, 850–866. https://doi.org/10.1016/j.seppur.2018.09.003.

Doulia, D., Leodopoulos, C., Gimouhopoulos, K. & Rigas, F. 2009 Adsorption of humic acid on acid-activated Greek bentonite. *Journal of Colloid and Interface Science* **340** (2), 131–141. https://doi.org/10.1016/j.jcis.2009.07.028.

dye|World dye variety 2020 *Acid Brown 354*. Available from: http://www.worlddyevariety.com/acid-dyes/acid-brown-354.html (accessed 2020).

Ejraei, A., Aroon, M. A. & Saravani, A. Z. 2019 Wastewater treatment using a hybrid system combining adsorption, photocatalytic degradation and membrane filtration processes. *Journal of Water Process Engineering* **28**, 45–53. https://doi.org/10.1016/j.jwpe.2019.01.003.

El-Ashtoukhy, E., Amin, N. & Abdel-Aziz, M. 2012 Decolorization of acid brown and reactive blue dyes by anodic oxidation in a batch recycle electrochemical reactor. *International Journal of Electrochemical Science* **7**, 11137–11148.

Fazlzadeh, M., Abdoallahzadeh, H., Khosravi, R. & Alizadeh, B. 2016 Removal of acid black 1 from aqueous solutions using $Fe_3O_4$ magnetic nanoparticles. *Journal of Mazandaran University of Medical Sciences* **26** (143), 172–184.

Frey, D. D., Engelhardt, F. & Greitzer, E. M. 2003 A role for 'one-factor-at-a-time' experimentation in parameter design. *Research in Engineering Design* **14** (2), 65–74. https://doi.org/10.1007/s00163-002-0026-9.

Gautam, R. & Chattopadhyaya, M. 2016 Chapter 5-kinetics and equilibrium isotherm modeling: graphene-based nanomaterials for the removal of heavy metals from water. In: *Nanomaterials for Wastewater Remediation* (R. K. Gautam & M. C. Chattopadhyaya, eds). Butterworth-Heinemann, Boston. https://doi.org/10.1016/B978-0-12-804609-8.00005-4.

Golizadeh, M., Karimi, A., Gandomi-Ravandi, S., Vossoughi, M., Khafaji, M., Joghataei, M. T. & Faghihi, F. 2019 Evaluation of cellular attachment and proliferation on different surface charged functional cellulose electrospun nanofibers. *Carbohydrate Polymers* **207**, 796–805. https://doi.org/10.1016/j.carbpol.2018.12.028.

Guo, S., Wu, K., Gao, Y., Liu, L., Zhu, X., Li, X. & Zhang, F. 2018 Efficient removal of Zn (II), Pb (II), and Cd (II) in waste water based on magnetic graphitic carbon nitride materials with enhanced adsorption capacity. *Journal of Chemical & Engineering Data* **63** (10), 3902–3912. https://doi.org/10.1021/acs.jced.8b00526.

Hamedi, A., Zarandi, M. B. & Nateghi, M. R. 2019 Highly efficient removal of dye pollutants by MIL-101 (Fe) metal-organic framework loaded magnetic particles mediated by Poly L-Dopa. *Journal of Environmental Chemical Engineering* **7** (1), 102882. https://doi.org/10.1016/j.jece.2019.102882.

Hameed, B. & Rahman, A. 2008 Removal of phenol from aqueous solutions by adsorption onto activated carbon prepared from biomass material. *Journal of Hazardous Materials* **160** (2–3), 576–581. https://doi.org/10.1016/j.jhazmat.2008.03.028.

Hashem, M. M. 2006 Development of a one-stage process for pretreatment and cationisation of cotton fabric. *Coloration Technology* **122** (3), 135–144. https://doi.org/10.1111/j.1478-4408.2006.00022.x.

Hassan, W., Noureen, S., Mustaqeem, M., Saleh, T. A. & Zafar, S. 2020 Efficient adsorbent derived from *Haloxylon recurvum* plant for the adsorption of acid brown dye: kinetics, isotherm and thermodynamic optimization. *Surfaces and Interfaces* **20**, 100510. https://doi.org/10.1016/j.surfin.2020.100510.

Ho, Y. & McKay, G. 1998 A comparison of chemisorption kinetic models applied to pollutant removal on various sorbents. *Process Safety and Environmental Protection* **76** (4), 332–340. https://doi.org/10.1205/095758298529696.

Ho, Y.-S., Chiu, W.-T. & Wang, C.-C. 2005 Regression analysis for the sorption isotherms of basic dyes on sugarcane dust. *Bioresource Technology* **96** (11), 1285–1291. https://doi.org/10.1016/j.biortech.2004.10.021.

Huang, H. P. & Jeng, J. C. 2005 Process reaction curve and relay methods identification and PID tuning. In: *PID Control: New Identification and Design Methods* (J. Crowe, K. K. Tan, T. H. Lee, R. Ferdous, M. R. Katebi, H. P. Huang, J. C. Jeng, K. S. Tang, G. R. Chen, K. F. Man, S. Kwong, A. Sánchez, Q. G. Wang, Y. Zhang, Y. Zhang, P. Martin, M. J. Grimble, D. R. Greenwood, M. A. Johnson & M. H. Moradi, eds). Springer London, London, pp. 297–337. doi:10.1007/1-84628-148-2_8.

Jarrah, A. & Farhadi, S. 2018 $K_6P_2W_{18}O_{62}$ encapsulated into magnetic $Fe_3O_4$/MIL-101 (Cr) metal–organic framework: a novel magnetically recoverable nanoporous adsorbent for ultrafast treatment of aqueous organic pollutants solutions. *RSC Advances* **8** (66), 37976–37992. https://doi.org/10.1039/C8RA06287 K.

Kałużna–Czaplińska, J., Gutowska, A. & Jóźwiak, W. K. 2010 The chemical degradation of C.I. acid brown 349 in aqueous solution using hydrogen peroxide and sodium hypochlorite and its implications for biodegradation. *Dyes and Pigments* **87**, 62–68. https://doi.org/10.1016/j.dyepig.2010.02.005.

Kamal, H., Abd-Elrahim, F. M. & Lotfy, S. 2014 Characterization and some properties of cellulose acetate-co-polyethylene oxide blends prepared by the use of gamma irradiation. *Journal of Radiation Research and Applied Sciences* **7** (2), 146–153. https://doi.org/10.1016/j.jrras.2014.01.003.

Katheresan, V., Kansedo, J. & Lau, S. Y. 2018 Efficiency of various recent wastewater dye removal methods: a review. *Journal of Environmental Chemical Engineering* **6** (4), 4676–4697. https://doi.org/10.1016/j.jece.2018.06.060.

Konicki, W., Sibera, D. & Narkiewicz, U. 2018 Adsorptive removal of cationic dye from aqueous solutions by ZnO/$ZnMn_2O_4$ nanocomposite. *Separation Science and Technology* **53** (9), 1295–1306. https://doi.org/10.1080/01496395.2018.1444054.

Li, G., Fu, Y., Shao, Z., Zhang, F. & Qin, M. 2015 Preparing cationic cellulose derivative in NaOH/urea aqueous solution and its performance as filler modifier. *BioResources* **10** (4), 7782–7794.

Lin, K.-Y. A. & Chang, H.-A. 2015 Ultra-high adsorption capacity of zeolitic imidazole framework-67 (ZIF-67) for removal of malachite green from water. *Chemosphere* **139**, 624–631. https://doi.org/10.1016/j.chemosphere.2015.01.041.

Liu, X., Gong, W., Luo, J., Zou, C., Yang, Y. & Yang, S. 2016 Selective adsorption of cationic dyes from aqueous solution by polyoxometalate-based metal–organic framework composite. *Applied Surface Science* **362**, 517–524. https://doi.org/10.1016/j.apsusc.2015.11.151.

Mahmoodi, N. M., Hayati, B. & Arami, M. 2012 Kinetic, equilibrium and thermodynamic studies of ternary system dye removal using a biopolymer. *Industrial Crops and Products* **35** (1), 295–301. https://doi.org/10.1016/j.indcrop.2011.07.015.

Morantes, D., Muñoz, E., Kam, D. & Shoseyov, O. 2019 Highly charged cellulose nanocrystals applied as a water treatment flocculant. *Nanomaterials* **9** (2), 272. doi: https://doi.org/10.3390/nano9020272.

Nasar, A. & Mashkoor, F. 2019 Application of polyaniline-based adsorbents for dye removal from water and wastewater – a review. *Environmental Science and Pollution Research* **26** (6), 5333–5356. https://doi.org/10.1007/s11356-018-3990-y.

Nasar, A. & Shakoor, S. 2017 Remediation of dyes from industrial wastewater using low-cost adsorbents. In: *Materials Research Foundations* (I. A. Al-Ahmed, ed.), pp. 1–33. http://dx.doi.org/10.21741/9781945291333-1.

Ofomaja, A. E. 2008 Sorptive removal of methylene blue from aqueous solution using palm kernel fibre: effect of fibre dose. *Biochemical Engineering Journal* **40** (1), 8–18. https://doi.org/10.1016/j.bej.2007.11.028.

Pal, S., Mal, D. & Singh, R. 2006 Synthesis, characterization and flocculation characteristics of cationic glycogen: a novel polymeric flocculant. *Colloids and Surfaces A: Physicochemical and Engineering Aspects* **289** (1–3), 193–199. https://doi.org/10.1016/j.colsurfa.2006.04.034.

Pandima Devi, M. & Muthukumaran, C. 2013 adsorption kinetics of acid brown dye from aqueous solution using biowaste. *Asian Journal of Science and Technology* **4** (8), 1–5.

Pansuk, C. & Vinitnantharat, S. 2011 A Comparative Study of the Adsorption of Acid Brown 75 and Direct Yellow 162 onto Unmodified and Surfactant Modified Granule Developed from Coal Fly Ash. In: *2nd International Conference on Environmental Science and Technology*, IACSIT Press, Singapore, pp. 49–54.

Piccin, J., Dotto, G. & Pinto, L. 2011 Adsorption isotherms and thermochemical data of FD&C Red n 40 binding by chitosan. *Brazilian Journal of Chemical Engineering* **28** (2), 295–304. https://doi.org/10.1590/S0104-66322011000200014.

Pielesz, A. & Biniaś, W. 2010 Cellulose acetate membrane electrophoresis and FTIR spectroscopy as methods of identifying a fucoidan in *Fucusvesiculosus* Linnaeus. *Carbohydrate Research* **345** (18), 2676–2682. https://doi.org/10.1016/j.carres.2010.09.027.

Rajasulochana, P. & Preethy, V. 2016 Comparison on efficiency of various techniques in treatment of waste and sewage water–a comprehensive review. *Resource-Efficient Technologies* **2** (4), 175–184. https://doi.org/10.1016/j.reffit.2016.09.004.

Raval, N. P., Shah, P. U. & Shah, N. K. 2016 Adsorptive amputation of hazardous azo dye congo red from wastewater: a critical review. *Environmental Science and Pollution Research* **23** (15), 14810–14853. https://doi.org/10.1007/s11356-016-6970-0.

Ruan, W., Hu, J., Qi, J., Hou, Y., Zhou, C. & Wei, X. 2019 Removal of dyes from wastewater by nanomaterials: a review. *Advanced Materials Letters* **10** (1), 9–20. https://doi.org/10.5185/amlett.2019.2148.

Saber-Samandari, S., Saber-Samandari, S., Joneidi-Yekta, H. & Mohseni, M. 2017 Adsorption of anionic and cationic dyes from aqueous solution using gelatin-based magnetic nanocomposite beads comprising carboxylic acid functionalized carbon nanotube. *Chemical Engineering*

*Journal* **308**, 1133–1144. https://doi.org/10.1016/j.cej.2016.10.017.

Saleh, T. A. 2011 The influence of treatment temperature on the acidity of MWCNT oxidized by $HNO_3$ or a mixture of $HNO_3/H_2SO_4$. *Applied Surface Science* **257** (17), 7746–7751. https://doi.org/10.1016/j.apsusc.2011.04.020.

Saleh, T. A. 2018 Simultaneous adsorptive desulfurization of diesel fuel over bimetallic nanoparticles loaded on activated carbon. *Journal of Cleaner Production* **172**, 2123–2132. https://doi.org/10.1016/j.jclepro.2017.11.208.

Saleh, T. A., Tuzen, M. & Sarı, A. 2018 Polyamide magnetic palygorskite for the simultaneous removal of Hg(II) and methyl mercury; with factorial design analysis. *Journal of Environmental Management* **211**, 323–333. https://doi.org/10.1016/j.jenvman.2018.01.050.

Salleh, M. A. M., Mahmoud, D. K., Karim, W. A. W. A. & Idris, A. 2011 Cationic and anionic dye adsorption by agricultural solid wastes: a comprehensive review. *Desalination* **280** (1–3), 1–13. https://doi.org/10.1016/j.desal.2011.07.019.

Seow, T. W. & Lim, C. K. 2016 Removal of dye by adsorption: a review. *International Journal of Applied Engineering Research* **11** (4), 2675–2679.

Song, Y.-L., Li, J.-T. & Chen, H. 2008 Removal of acid brown 348 dye from aqueous solution by ultrasound irradiated exfoliated graphite. *Indian Journal of Chemical Technology* **15**, 443–448.

Teh, C. Y., Budiman, P. M., Shak, K. P. Y. & Wu, T. Y. 2016 Recent advancement of coagulation–flocculation and its application in wastewater treatment. *Industrial & Engineering Chemistry Research* **55** (16), 4363–4389. https://doi.org/10.1021/acs.iecr.5b04703.

Togue Kamga, F. 2018 Modeling adsorption mechanism of paraquat onto ayous (*Triplochiton scleroxylon*) wood sawdust. *Applied Water Science* **9** (1), 1. doi: 10.1007/s13201-018-0879-3.

Wang, T., Zhao, P., Lu, N., Chen, H., Zhang, C. & Hou, X. 2016 Facile fabrication of $Fe_3O_4$/MIL-101 (Cr) for effective removal of acid red 1 and orange G from aqueous solution. *Chemical Engineering Journal* **295**, 403–413. https://doi.org/10.1016/j.cej.2016.03.016.

Wu, J.-S., Liu, C.-H., Chu, K. H. & Suen, S.-Y. 2008 Removal of cationic dye methyl violet 2B from water by cation exchange membranes. *Journal of Membrane Science* **309** (1–2), 239–245. https://doi.org/10.1016/j.memsci.2007.10.035.

Yagub, M. T., Sen, T. K., Afroze, S. & Ang, H. M. 2014 Dye and its removal from aqueous solution by adsorption: a review. *Advances in Colloid and Interface Science* **209**, 172–184. https://doi.org/10.1016/j.cis.2014.04.002.

Yaseen, D. A. & Scholz, M. 2019 Textile dye wastewater characteristics and constituents of synthetic effluents: a critical review. *International Journal of Environmental Science and Technology* **16** (2), 1193–1226. doi: 10.1007/s13762-018-2130-z.

First received 1 September 2020; accepted in revised form 4 February 2021. Available online 17 February 2021